In vivo delivery of an exogenous molecule into murine T lymphocytes using a lymphatic drug delivery system combined with sonoporation

doi: 10.1016/j.bbrc.2020.02.174

In Vivo Delivery of an Exogenous Molecule into Murine T Lymphocytes using a Lymphatic Drug Delivery System Combined with Sonoporation

Shigeki Kato[1, 2, 3], Yuko Shirai[2, 3], Chihiro Motozono[4], Hiroyuki Kanzaki[5], Shiro Mori[2, 3, 6], Tetsuya Kodama[2, 3, 7]*

[1] Department of Immunology, Kindai University Faculty of Medicine, Osaka-Sayama, Osaka 589-8511, Japan

[2] Laboratory of Biomedical Engineering for Cancer, Graduate School of Biomedical Engineering, Tohoku University, 4-1 Seiryo, Aoba, Sendai, Miyagi 980-8575, Japan

[3] Biomedical Engineering Cancer Research Center, Graduate School of Biomedical Engineering, Tohoku University, 4-1 Seiryo, Aoba, Sendai, Miyagi 980-8575, Japan

[4] Department of Molecular Immunology, Research Institute for Microbial Diseases, Osaka University, Osaka 565-0871, Japan

[5] Department of Orthodontics, School of Dental Medicine, Tsurumi University, 2-1-3 Tsurumi, Tsurumi-ku, Yokohama 230-8501, Japan

[6] Department of Oral and Maxillofacial Surgery, Tohoku University Hospital, 1-1 Seiryo, Aoba, Sendai, Miyagi 980-8575, Japan

[7] Department of Electronic Engineering, Graduate School of Engineering, Tohoku University, 980-8579, Japan

Corresponding author: Tetsuya Kodama, PhD (Eng.), PhD (Med.), Laboratory of Biomedical Engineering for Cancer, Graduate School of Biomedical Engineering, Tohoku University, 4-1 Seiryo, Aoba, Sendai, Miyagi 980-8575, Japan.

Tel & Fax: +81-22-717-7583; E-mail: kodama@tohoku.ac.jp

Abstract

Physical delivery of exogenous molecules into lymphocytes is extremely challenging because conventional methods have notable limitations. Here, we evaluated the potential use of acoustic liposomes (ALs) and sonoporation to deliver exogenous molecules into lymphocytes within a lymph node (LN). MXH10/Mo-*lpr*/*lpr* (MXH10/Mo/lpr) mice, which show systemic LN swelling, were used as the model system. After direct injection into the subiliac LN, a solution containing both ALs and TOTO-3 fluorophores (molecular weight: 1,355) was able to reach the downstream proper axillary LN (PALN) via the lymphatic vessels (LVs). This led to the accumulation of a high concentration of TOTO-3 fluorophores and ALs in the lymphatic sinuses of the PALN, where a large number of lymphocytes were densely packed. Exposure of the PALN to >1.93 W/cm^2 of 970-kHz ultrasound allowed the solution to extravasate into the parenchyma and reach the large number of lymphocytes in the sinuses. Flow cytometric analysis showed that TOTO-3 molecules were delivered into 0.49 ± 0.23% of $CD8^+7AAD^-$ cytotoxic T lymphocytes. Furthermore, there was no evidence of tissue damage. Thus, direct administration of drugs into LVs combined with sonoporation can improve the delivery of exogenous molecules into primary lymphocytes. This technique could become a novel approach to immunotherapy.

Keywords

Cavitation; Drug delivery; Ultrasound; Acoustic liposome; Lymphocyte; Immunotherapy

1. Introduction

Immune cells protect the body against microbial threats and eliminate mutated cells, thus immune system dysfunction leads to serious diseases. For example, $CD8^+$ cytotoxic T lymphocytes (CTLs) are major effectors in the elimination of cells that have mutated due to infection or cancer. However, functional disorders of CTLs result in disease exacerbation [1]. The delivery of exogenous therapeutic macromolecules such as DNA, peptides and siRNA into CTLs could potentially facilitate a recovery of normal function, allowing these cells to overcome several important diseases. Although viral vectors have been used for gene delivery into lymphocytes, this approach has considerable disadvantages that include the use of a potential biohazard and the risk of secondary tumor development [2]. Physical approaches such as electroporation, photoporation and ballistic transfer have been evaluated as alternative techniques for delivering exogenous molecules into lymphocytes [3-5]. However, these conventional physical methods were associated with poor delivery efficiency, in part because they were performed in an environment containing insufficient lymphocytes [6,7].

Ultrasound (US)-mediated delivery of molecules into living cells (sonoporation) is an alternative technique to viral vector methods or electroporation [8,9]. Low-intensity US-driven oscillation of lipid-shelled gas bubbles can generate mechanical pressures such as microstreaming-shear stress or impulsive jets (i.e., stable cavitation). These mechanical pressures create a resealing pore on the plasma membrane of a target cell and stimulate endocytosis, thereby facilitating delivery of a membrane-impermeant agent into the cytoplasm or nucleus [10,11]. Under more intense US conditions, the bubbles undergo violent oscillations and sudden collapse to create localized surface damage (i.e., inertial

cavitation) [12]. These mechanical pressures can also loosen endothelial cell junctions, promoting the leakage of components from vessels [13]. Since the mechanical stresses only affect cells or tissues within the US-irradiated area, sonoporation-driven drug delivery can achieve tissue selectivity without evoking an immune response or systemic inflammation.

Previously, we demonstrated that a lymphatic drug delivery system (LDDS) was able to directly deliver drugs into the lymphatic system of the MXH10/Mo-*lpr*/*lpr* (MXH10/Mo/lpr) mouse, which exhibits systemic lymph node (LN) swelling. This approach has great potential as a method for internalizing drugs into cells that reside in LNs [14-16]. Solutions injected into the subiliac LN (SiLN) by the LDDS were able to flow into the efferent lymphatic vessels (LVs) and reach the downstream proper axillary LN (PALN) [17-19]. Therefore, the LDDS potentially could be used to deliver high concentrations of therapeutic drugs and acoustic liposomes (ALs, which act as cavitation nuclei) into the sinuses of the PALN where lymphocytes are densely packed. If sonoporation-generated mechanical pressures were able to change the structure of lymphatic endothelial cell junctions, a solution administered by a LDDS would be extravasated into the parenchyma, allowing many lymphocytes to come into contact with high local concentrations of drugs administered with the ALs. In the US field, leaked ALs and their gas vesicles would collapse or act as cavitation nuclei to increase the membrane permeability of the lymphocytes, thereby facilitating drug internalization into the targeted lymphocytes.

In the present study, we investigated whether the combined use of a LDDS and sonoporation (with ALs) could be used to deliver an exogenous molecule, namely

TOTO-3 fluorophore, into the LN cells of MXH10/Mo/lpr mice. Furthermore, we evaluated the efficiency of drug delivery into $CD8^+$ T cells using immunofluorescence staining of LNs and flow cytometry.

2. Materials and Methods

Experiments were carried out in accordance with published guidelines and approved by the Institutional Animal Care and Use Committee of Tohoku University. The number of mice used was kept to a minimum for bioethical reasons.

2.1. Mice

The MXH10/Mo/lpr mouse, a sub-line of the MXH/lpr mouse obtained by intercrossing MRL/MpJ-*lpr*/*lpr* and C3H/HeJ-*lpr*/*lpr* strains, develops systemic swelling of LNs (up to 10 mm in diameter, similar in size to human LNs) at only 14 weeks of age. MXH10/Mo/lpr mice (aged 14–18 weeks) were bred under specific pathogen-free conditions in the Animal Research Institute, Graduate School of Medicine, Tohoku University, Sendai, Japan.

For anatomical experiments, BALB/c mice (aged 10 weeks; CLEA Japan, Tokyo, Japan) were used for comparisons of LN sizes.

2.2. ALs

ALs were prepared as previously described [20].

2.3. Identification of LNs

One BALB/c mouse was used for identification of LNs. The mouse was euthanized after the injection of 10 μL trypan blue dye into the forepaw, and an incision was made in the ipsilateral axillary region. The subcutaneous connective tissue was separated to free the skin flap and expose the LVs and LNs located in the axillary region, taking care not to injure these structures.

One BALB/c mouse and one MXH10/Mo/lpr mouse were used to visualize and measure the volume of the PALN with high-frequency US imaging (HF-US). The mouse was anesthetized and positioned on a heated stage. The scanner was equipped with a mechanical single-element transducer (RMV708 for the BALB/c mouse: central frequency, 55 MHz; axial resolution, 30 μm; lateral resolution, 70 μm; focal length, 4.5 mm; depth of field, 1.4 mm; RMV-710B for the MXH10/Mo/lpr mouse: central frequency, 25 MHz; axial resolution, 70 μm; lateral resolution, 140 μm; focal length, 15 mm; depth of field, 2.7 mm; VisualSonics, Toronto, ON, Canada). The B-mode images were reconstructed into a 3D image, and the volume (consisting of multiple polygons) was calculated using Vevo 770 software (VisualSonics) [15].

2.4. Delivery of TOTO-3 using a LDDS and sonoporation

The delivery of TOTO-3 from the SiLN to the PALN via LVs was carried out as previously described [15], and the experimental setup is shown in **Fig. 1B**. Briefly, 200 μL of solution containing 100 μL ALs and 100 μL TOTO-3 fluorophore (T-3604; Molecular Probes, Eugene, OR, USA; molecular weight: 1,355; absorption: 642 nm; emission: 660 nm) was injected into the SiLN through a butterfly needle (Terumo, Tokyo,

Japan). A 970-kHz flat, disk-shaped and submersible US transducer with a diameter of 12 mm (Honda Electronics, Toyohashi, Japan) was placed in contact with the PALN, and the PALN was exposed to non-focused US. US calibration was carried out, and the spatial peak-temporal average of the US intensity (I_{SPTA}) was calculated as previously described [14-16]. The duty ratio was 20%, the exposure time was 60 s, and the number of cycles in the pulse was 200 [21]. A total of 16 mice were used (4 mice for each experimental condition).

2.5. Immunofluorescence and staining with hematoxylin-eosin (HE)

To observe the PALN region into which TOTO-3 was delivered and evaluate tissue damage, immunofluorescence on frozen sections and staining with HE were performed using standard protocols [15,16]. Each mouse was deeply anesthetized and euthanized after sonication. The PALN was extracted and embedded in optimal cutting temperature (OCT) compound (Sakura Fineteck Japan, Tokyo, Japan), and frozen samples were sectioned (10-μm thickness) with a cryostat (Thermo Fisher Scientific, Barrington, IL, USA). The sections were fixed in paraformaldehyde (Wako Pure Chemical Industries, Ltd., Osaka, Japan) at room temperature for 20 min, and nuclei were stained with 100 ng/mL 4',6-diamino-2-phenylindole (DAPI; Sigma-Aldrich, St. Louis, MO, USA) at room temperature. Lymphatic endothelia were detected using rabbit anti-lymphatic vessel endothelial hyaluronan receptor-1 (LYVE-1) primary antibody (ReliaTech GmbH, Wolfenbüttel, Germany) and Alexa-488-conjugated goat anti-rabbit secondary antibody (Invitrogen, Carlsbad, CA, USA). Images revealing DAPI (excitation: 405 nm, emission: 400–450 nm), Alexa-488 (excitation: 496 nm, emission: 519 nm) and TOTO-3

(excitation: 635 nm, emission: 660 nm) fluorescence were captured using a fluorescence microscope (BX51, Olympus, Tokyo, Japan).

2.6. Flow cytometric analysis of TOTO-3 delivered to lymphocytes

Flow cytometric analysis of cell-surface markers was carried out to identify lymphocytes into which TOTO-3 had been delivered. PALN tissue was dissociated in cold Dulbecco's phosphate-buffered saline (PBS; Sigma-Aldrich), and a single-cell suspension was prepared by passing the dissociated tissue through a wire cloth. Cells were stained with phycoerythrin-conjugated anti-mouse CD8 monoclonal antibody (rat IgG2a; BioLegend, San Diego, CA, USA) for 20 min on ice, washed three times with PBS containing 2% heat-inactivated fetal bovine serum (HyClone Laboratories Inc., South Logan, Utah, USA) and stained with 20 μg/mL 7-aminoactinomycin D (7-AAD; BioLegend) to exclude dead cells. Multicolor flow cytometric analyses were performed with an Accuri C6 cytometer (Becton Dickinson Immunocytometry Systems, San Jose, CA, USA).

2.7. Data analysis

Two independent experiments were carried out for the flow cytometric analyses, and a ratio or mean fluorescence intensity (MFI) was calculated for $TOTO3^{+}CD8^{+}7AAD^{-}$ cells. Two mice were used for each independent experiment, one for PBS alone and the other for TOTO-3 + ALs + US. Data are presented as the mean ± standard deviation (s.d.). Graphs were constructed using Excel for Windows (Microsoft Corp., Redmond, WA, USA).

3. Results and Discussion

As LNs are difficult to identify by the naked eye in a typical experimental mouse such as the BALB/c species, trypan blue dye was injected into the forepaw to highlight them. **Figure 1A** shows the gross anatomy of the BALB/c mouse after the injection of trypan blue dye. The dashed circle and triangles in the enlarged image represent the draining LN from the ipsilateral forepaw. By contrast, the LNs of MXH10/Mo/lpr mice could be clearly identified (**Fig. 1B**). It was straightforward to inject solutions into the SiLN of the MXH10/Mo/lpr mouse, and this LN was connected by LVs to a downstream LN (the PALN).

To compare LN volume between species, a HF-US imaging system was used to construct a 3D image of each LN and calculate its volume. The PALN volumes of BALB/c and MXH10/Mo/lpr mice were 0.85 mm^3 (**Fig. 1C**) and 430.3 mm^3 (**Fig. 1D**), respectively. LN volume was approximately 500 times greater in the MXH10/Mo/lpr mouse than in the BALB/c mouse, which enabled solutions to be administered accurately into the LN of the MXH10/Mo/lpr mouse.

Lymphocytes that differentiated in the bone marrow circulate throughout the body via blood vessels, during which time they also temporarily reside in LNs [22]. Since LNs are rich in lymphocytes, they are good candidate targets for the delivery of molecules into lymphocytes. Superficial LNs are well suited for US-mediated molecular delivery into lymphocytes because their superficial position minimizes US energy attenuation. **Figure 1B** illustrates a schematic view of the sonoporation technique. When a mixture of TOTO-3 fluorophores and ALs was injected into the SiLN, the solution drained into the efferent LVs and entered the downstream PALN [19]. The use of this LDDS enables the downstream LN's sinuses, which contain a large number of lymphocytes, to become filled

with the injected solution [23]. When one considers the structure of the endothelial wall, the delivery window is larger for lymphatic endothelia (10–100 nm) than for blood capillaries (< 10 nm) [24], meaning that drugs could potentially be delivered to lymphocytes residing adjacent to the sinuses. If this was achieved, mechanical pressures derived from sonoporation might promote the efficient delivery of drug into the lymphocytes. To test this hypothesis, immunofluorescence staining experiments were carried out after LDDS-mediated administration of TOTO-3 and ALs with/without exposure to US (**Fig. 2A**). Nuclei were stained blue, lymphatic endothelia were stained green, and the red area represents TOTO-3 that had been delivered to nuclei. TOTO-3 signals were not detected in the negative control group. Only a weak TOTO-3 signal was detected in the marginal sinuses when 0.29 W/cm^2 of US was applied to the PALN after the administration of TOTO-3 and ALs (**Fig. 2B**). However, a strong signal was detected both in the peripheral marginal sinuses and inner lymphatic sinuses when 1.98 or 2.93 W/cm^2 of US was applied to the PALN (**Fig. 2C**). Sonication of the PALN might lead to the collapse of ALs and generation of cavitation bubbles that induce mechanical pressures [14,16]. Cavitation bubbles near the rigid, lymphatic endothelial junctions may collapse asymmetrically to form impulsive jets that change the endothelial structure and thereby loosen the endothelial junctions [25]. Consequently, the mixture of TOTO-3 molecules and AL-derived gas vesicles would be able to extravasate into the lymphatic parenchyma where lymphocytes are densely distributed. The extravasated gas vesicles would inevitably be transported to adjacent lymphocytes, and further sonication would generate growing cavitations that would enhance cell membrane permeability and thereby promote the efficient uptake of TOTO-3 into lymphocytes.

Next, to demonstrate that exogenous molecules could be internalized into lymphocyte nuclei without tissue or cellular damage, HE-stained frozen sections of the PALN were evaluated for any signs of tissue injury or cytotoxicity after sonoporation (**Fig. 3)**. When compared with non-sonicated PALN (PBS alone), sonication resulted in no collapse or abnormalities of the intralymphatic structures, including the capsule and marginal sinus, even when high-intensity US was applied to the PALN (TOTO-3 + AL + US (2.93 W/cm^2)). This means that the effects of cavitation were transient phenomena and that the lymphatic endothelial cell junctions resealed after sonication. In addition, evidence for cellular damage such as nuclear fragmentation was not observed in sonicated samples.

Finally, we investigated the delivery of TOTO-3 molecules into CTLs after sonoporation using 2.93 W/cm^2 of US. **Figure 4A** shows the representative gating scheme for the flow cytometric analysis of cells isolated from the PALN. For the detection of TOTO-3 positive cells, the threshold was set as zero in the PBS alone group (**Fig. 4B upper panels**). Thus, TOTO-3 fluorescence was not detected in the PBS alone group. In two independent experiments, TOTO-3 was delivered into 0.33% and 0.65% of CTLs (TOTO-$3^+CD8^+7AAD^-$), and the average was 0.49 ± 0.23% (**Fig. 4B lower panels and 4C**). The MFI of the TOTO-$3^+CD8^+7AAD^-$ cells was 2680 and 5383, respectively, and the average was 4031 ± 1911 (**Fig. 4B lower panels and 4D**).

Previous studies have reported that several types of exogenous molecules can be delivered into lymphocytes by sonoporation *in vitro* [26,27]. To the best of our knowledge, the present study is the first to demonstrate that exogenous molecules can be delivered into non-dividing primary T lymphocytes *in vivo* by combining a LDDS with sonoporation. Recently, Karki et al. [28] reported that siRNA (MW: 14 kDa) delivery into murine and

human primary T lymphocytes was facilitated by sonoporation, and the delivered siRNA was able to regulate lymphocyte function *in vitro*. These interesting findings indicate that mechanical stresses or impulsive pressures derived from sonoporation allow a relatively large molecule to internalize into the cytoplasm of living primary lymphocytes. In addition, macromolecules of 20 MDa could be extravasated from the vessels and distributed into the extracellular matrix by sonoporation [29]. We have shown that an impermeant molecule with a relatively large size can be delivered into primary lymphocytes in LNs using a LDDS and sonoporation.

In conclusion, we report a new method of delivering exogenous molecules into mouse lymphocytes *in vivo* using lymphatic administration combined with sonoporation. After the injection of solution containing TOTO-3 and ALs into the SiLN of the MXH10/Mo/lpr mouse, the solution drained into the downstream PALN via LVs to accumulate at a high concentration in the sinuses where the target lymphocytes were densely packed. Under these conditions, strong TOTO-3 fluorescence signals were detected around the marginal and lymphatic sinuses of the PALN after US was applied at intensities >1.93 W/cm^2, whereas weak TOTO-3 signals were observed when an US intensity of 0.29 W/cm^2 was used. Furthermore, flow cytometry revealed that TOTO-3 was delivered into CTLs near the sinuses. Although these data indicate that the combined use of a LDDS with sonoporation could enhance the delivery of exogenous molecules into primary lymphocytes, further studies are required to investigate the functions of T lymphocytes after the delivery of real therapeutic agents instead of TOTO-3.

Acknowledgements

This study was supported in part by JSPS KAKENHI grant numbers 26293425 (SM), 16K15816 (SM), 26242051 (TK), 17H00865 (TK), 17K20077 (TK), 19K22941 (TK), 17K13039 (SK) and 19K16622 (SK). The authors would like to thank T. Sato for technical assistance.

References

[1] S. Takamura, S. Tsuji-Kawahara, H. Yagita, H. Akiba, M. Sakamoto, T. Chikaishi, M. Kato, M. Miyazawa, Premature terminal exhaustion of Friend virus-specific effector CD8+ T cells by rapid induction of multiple inhibitory receptors, J Immunol, 184 (2010) 4696-4707.

[2] C. Goffinet, O.T. Keppler, Efficient nonviral gene delivery into primary lymphocytes from rats and mice, FASEB J, 20 (2006) 500-502.

[3] U.K. Tirlapur, K. Konig, Targeted transfection by femtosecond laser, Nature, 418 (2002) 290-291.

[4] T. Kodama, M.R. Hamblin, A.G. Doukas, Cytoplasmic molecular delivery with shock waves: importance of impulse, Biophys J, 79 (2000) 1821-1832.

[5] Y. Cao, E. Ma, S. Cestellos-Blanco, B. Zhang, R. Qiu, Y. Su, J.A. Doudna, P. Yang, Nontoxic nanopore electroporation for effective intracellular delivery of biological macromolecules, Proc Natl Acad Sci U S A, 116 (2019) 7899-7904.

[6] C.E. Thomas, A. Ehrhardt, M.A. Kay, Progress and problems with the use of viral vectors for gene therapy, Nat Rev Genet, 4 (2003) 346-358.

[7] M.P. Stewart, A. Sharei, X. Ding, G. Sahay, R. Langer, K.F. Jensen, In vitro and ex vivo strategies for intracellular delivery, Nature, 538 (2016) 183-192.

[8] M. Fechheimer, J.F. Boylan, S. Parker, J.E. Sisken, G.L. Patel, S.G. Zimmer, Transfection of mammalian cells with plasmid DNA by scrape loading and sonication loading, Proc Natl Acad Sci U S A, 84 (1987) 8463-8467.

[9] Z. Cao, T. Zhang, X. Sun, M. Liu, Z. Shen, B. Li, X. Zhao, H. Jin, Z. Zhang, Y. Tian, Membrane-permeabilized sonodynamic therapy enhances drug delivery into macrophages, PLoS One, 14 (2019) e0217511.

[10] K. Tachibana, T. Uchida, K. Ogawa, N. Yamashita, K. Tamura, Induction of cell-membrane porosity by ultrasound, Lancet, 353 (1999) 1409.

[11] S. Hernot, A.L. Klibanov, Microbubbles in ultrasound-triggered drug and gene delivery, Adv Drug Deliv Rev, 60 (2008) 1153-1166.

[12] S. Xu, D. Ye, L. Wan, Y. Shentu, Y. Yue, M. Wan, H. Chen, Correlation Between Brain Tissue Damage and Inertial Cavitation Dose Quantified Using Passive Cavitation Imaging, Ultrasound Med Biol, 45 (2019) 2758-2766.

[13] P. Qin, T. Han, A.C.H. Yu, L. Xu, Mechanistic understanding the bioeffects of ultrasound-driven microbubbles to enhance macromolecule delivery, J Control Release, 272 (2018) 169-181.

[14] S. Kato, Y. Shirai, M. Sakamoto, S. Mori, T. Kodama, Use of a Lymphatic Drug Delivery System and Sonoporation to Target Malignant Metastatic Breast Cancer Cells

Proliferating in the Marginal Sinuses, Sci Rep, 9 (2019) 13242.

[15] S. Kato, Y. Shirai, H. Kanzaki, M. Sakamoto, S. Mori, T. Kodama, Delivery of molecules to the lymph node via lymphatic vessels using ultrasound and nano/microbubbles, Ultrasound Med Biol, 41 (2015) 1411-1421.

[16] S. Kato, S. Mori, T. Kodama, A Novel Treatment Method for Lymph Node Metastasis Using a Lymphatic Drug Delivery System with Nano/Microbubbles and Ultrasound, J Cancer, 6 (2015) 1282-1294.

[17] L. Shao, K. Takeda, S. Kato, S. Mori, T. Kodama, Communication between lymphatic and venous systems in mice, J Immunol Methods, 424 (2015) 100-105.

[18] L. Shao, S. Mori, Y. Yagishita, T. Okuno, Y. Hatakeyama, T. Sato, T. Kodama, Lymphatic mapping of mice with systemic lymphoproliferative disorder: usefulness as an inter-lymph node metastasis model of cancer, J Immunol Methods, 389 (2013) 69-78.

[19] T. Kodama, Y. Hatakeyama, S. Kato, S. Mori, Visualization of fluid drainage pathways in lymphatic vessels and lymph nodes using a mouse model to test a lymphatic drug delivery system, Biomed Opt Express, 6 (2015) 124-134.

[20] N. Sax, T. Kodama, Optimization of acoustic liposomes for improved in vitro and in vivo stability, Pharm Res, 30 (2013) 218-224.

[21] T. Kodama, A. Aoi, Y. Watanabe, S. Horie, M. Kodama, L. Li, R. Chen, N. Teramoto, H. Morikawa, S. Mori, M. Fukumoto, Evaluation of transfection efficiency in skeletal muscle using nano/microbubbles and ultrasound, Ultrasound Med Biol, 36 (2010) 1196-1205.

[22] J.P. Girard, C. Moussion, R. Forster, HEVs, lymphatics and homeostatic immune cell trafficking in lymph nodes, Nat Rev Immunol, 12 (2012) 762-773.

[23] T. Kodama, D. Matsuki, A. Tada, K. Takeda, S. Mori, New concept for the prevention and treatment of metastatic lymph nodes using chemotherapy administered via the lymphatic network, Sci Rep, 6 (2016) 32506.

[24] H. Fujii, S. Horie, K. Takeda, S. Mori, T. Kodama, Optimal range of injection rates for a lymphatic drug delivery system, J Biophotonics, 11 (2018) e201700401.

[25] P. Prentice, A. Cuschieri, K. Dholakia, M. Prausnitz, P. Campbell, Membrane disruption by optically controlled microbubble cavitation, Nature Physics, 1 (2005) 107-110.

[26] J. Wu, J. Pepe, M. Rincon, Sonoporation, anti-cancer drug and antibody delivery using ultrasound, Ultrasonics, 44 Suppl 1 (2006) e21-25.

[27] N. Jiang, Q. Chen, S. Cao, B. Hu, Y.J. Wang, Q. Zhou, R.Q. Guo, Ultrasoundtargeted microbubbles combined with a peptide nucleic acid binding nuclear localization signal

mediate transfection of exogenous genes by improving cytoplasmic and nuclear import, Mol Med Rep, 16 (2017) 8819-8825.

[28] A. Karki, E. Giddings, A. Carreras, D. Champagne, K. Fortner, M. Rincon, J. Wu, Sonoporation as an Approach for siRNA delivery into T cells, Ultrasound Med Biol, 45 (2019) 3222-3231.

[29] P.T. Yemane, A.K.O. Aslund, S. Snipstad, A. Bjorkoy, K. Grendstad, S. Berg, Y. Morch, S.H. Torp, R. Hansen, C.L. Davies, Effect of Ultrasound on the Vasculature and Extravasation of Nanoscale Particles Imaged in Real Time, Ultrasound Med Biol, 45 (2019) 3028-3041.

Figure Legends

Figure 1. Identification of LNs in BALB/c mice (A, C) and MXH10/Mo/lpr mice (B, D). Panel A shows the gross anatomy of a BALB/c mouse (female, 10 weeks of age) after the injection of trypan blue dye. The arrow indicates the injection site. The dashed outline and triangles in the enlarged picture indicate the draining LN from the ipsilateral forepaw. After 3D reconstruction using a high-frequency US imaging system, the volume of the PALN was calculated to be 0.85 mm^3 (C). In contrast, the LNs in an MXH10/Mo/lpr mouse (female, 14 weeks of age) could be clearly identified (B), and the volume of the LN was calculated to be 430.3 mm^3 (D), a volume more than 500 times greater than that in the BALB/c mouse. For delivery of TOTO-3 by lymphatic administration combined with sonoporation, a mixture of TOTO-3 and ALs was injected into the SiLN through a butterfly needle and flowed into the LVs at a rate of 50 μL/min. Solution entered the PALN from the afferent LVs and subsequently flowed into the marginal sinuses of the LNs. After finishing the administration, the US transducer surface was covered with liquid gel and positioned on the superficial skin at the PALN. Subsequently, US was applied to the PALN for 60 s. US signals were generated by a multifunction synthesizer and amplified by a bipolar amplifier. The US wave output was monitored on an oscilloscope. These procedures were carried out with mice under deep anesthesia.
ALs: acoustic liposomes, LN: lymph node, SiLN: subiliac LN, PALN: proper axillary LN, LVs: lymphatic vessels.

Figure 2. TOTO-3 localization in the PALN after sonoporation. (A) To detect the region of the PALN to which TOTO-3 had been delivered, immunofluorescence staining of sections was performed. Nuclei were stained blue (DAPI), and lymphatic endothelia were

stained green. The red area represents nuclei to which TOTO-3 had been delivered. TOTO-3 signals were not detected in the negative control group. When 0.29 W/cm^2 of US was applied to the PALN after the administration of TOTO-3 with ALs, a small amount of TOTO-3 signal was detected in the marginal sinuses (triangles). When 1.98 or 2.93 W/cm^2 of US was applied to the PALN, a strong signal intensity was detected in not only the peripheral marginal sinus but also the inner lymphatic sinuses. (B, C) Immunofluorescence on frozen sections of the PALN after 0.29 W/cm^2 or 1.98 W/cm^2 of US had been applied to the PALN. Images showing LYVE-1-positive lymphatic endothelia (green) and TOTO-3 delivered to lymphocytes (red) have been overlaid. Yellow regions are positive for both LYVE-1 and TOTO-3. Only a small amount of TOTO-3 signal was detected for an US intensity of 0.29 W/cm^2 (*), whereas strong TOTO-3 signals were observed for an US intensity of 1.98 W/cm^2 (arrows). Bar represents 100 μm.

Figure 3. Evaluation of tissue or cellular damage in the PALN after sonoporation. In the PBS alone group (n = 4), PBS was administered into the SiLN, and US treatment was not carried out. In the TOTO-3 + AL + US group (n = 4), TOTO-3 fluorophores and ALs were injected together into the SiLN, and 2.93 W/cm^2 of US was applied to the PALN after finishing the administration of the agents. The mice were euthanized after treatment, and the PALN was resected, embedded in OCT compound and frozen in liquid nitrogen. Frozen samples were sectioned (10 μm) and stained with HE to evaluate potential tissue damage caused by sonication. Lymphatic structures such as the capsule and marginal sinus were maintained, and no necrotic or apoptotic areas were detected in both the PBS alone and TOTO-3 + AL + US groups.

Figure 4. Flow cytometric analysis of TOTO-3 delivery into lymphocytes when 2.93 W/cm^2 of US was applied to the PALN following the lymphatic administration of TOTO-3 with ALs. (A) Representative gating strategy for $CD8^+$ T lymphocytes. Dead cells were eliminated using 7AAD. $CD8^+$ lymphocytes were gated on $CD8^+$ $7AAD^-$. For detection of TOTO-3-positive cells, the threshold of the TOTO-3 negative population was set as the maximum fluorescence intensity in PBS alone (B). The percentage of $CD8^+$ T lymphocytes containing TOTO-3 was 0.49 ± 0.23% (C). The mean fluorescence intensity in the TOTO-3 + AL + US group (administration of TOTO-3 and ALs followed by sonication with US) was 4031 ± 1911, whereas the value in the PBS alone group (administration of PBS into the SiLN but no sonication) was zero (D). Error bar represents ± s.d.

Figure 1

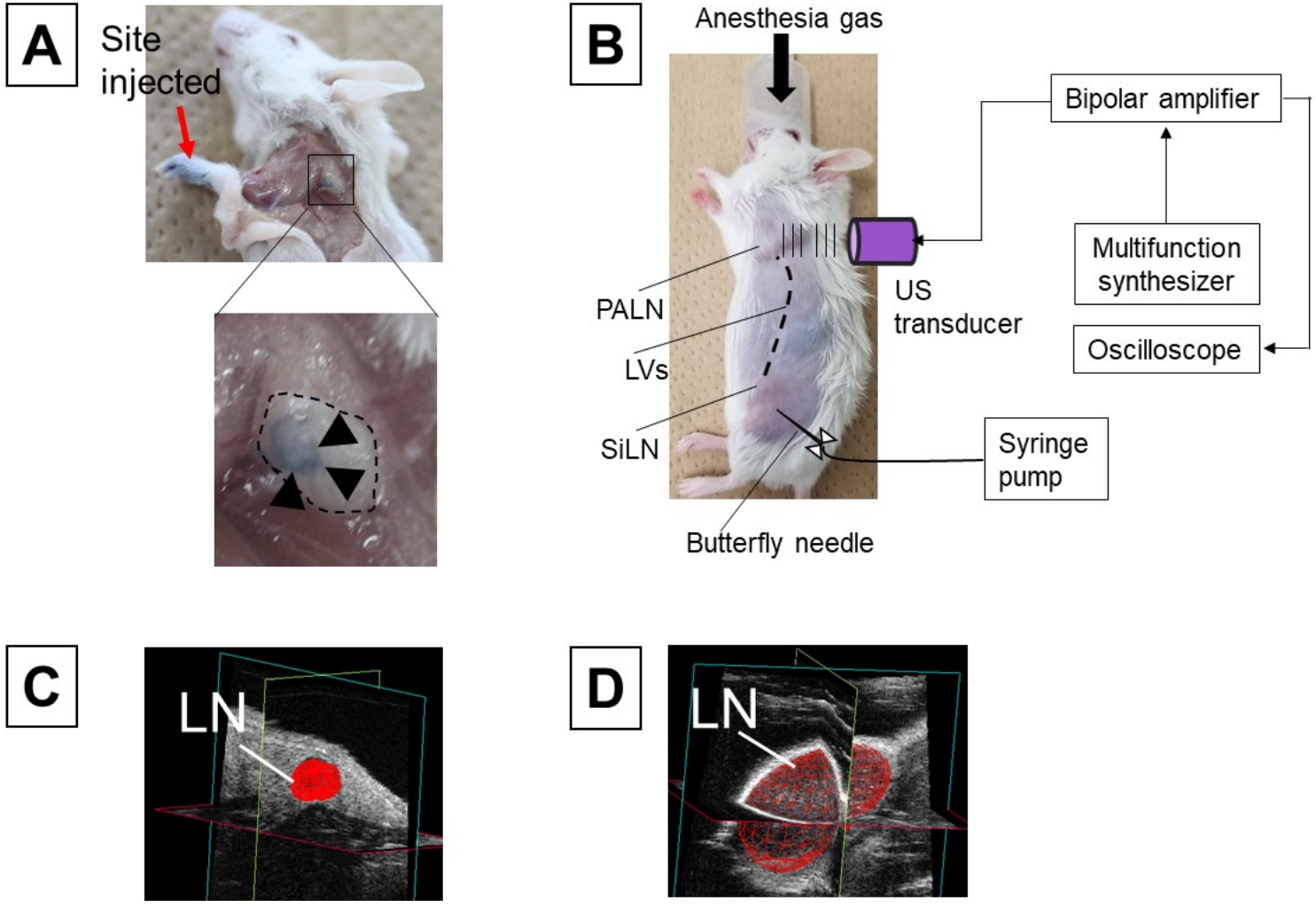
A
Site injected
B
Anesthesia gas
Bipolar amplifier
Multifunction synthesizer
Oscilloscope
US transducer
PALN
LVs
SiLN
Syringe pump
Butterfly needle
C
LN
D
LN

Figure 2

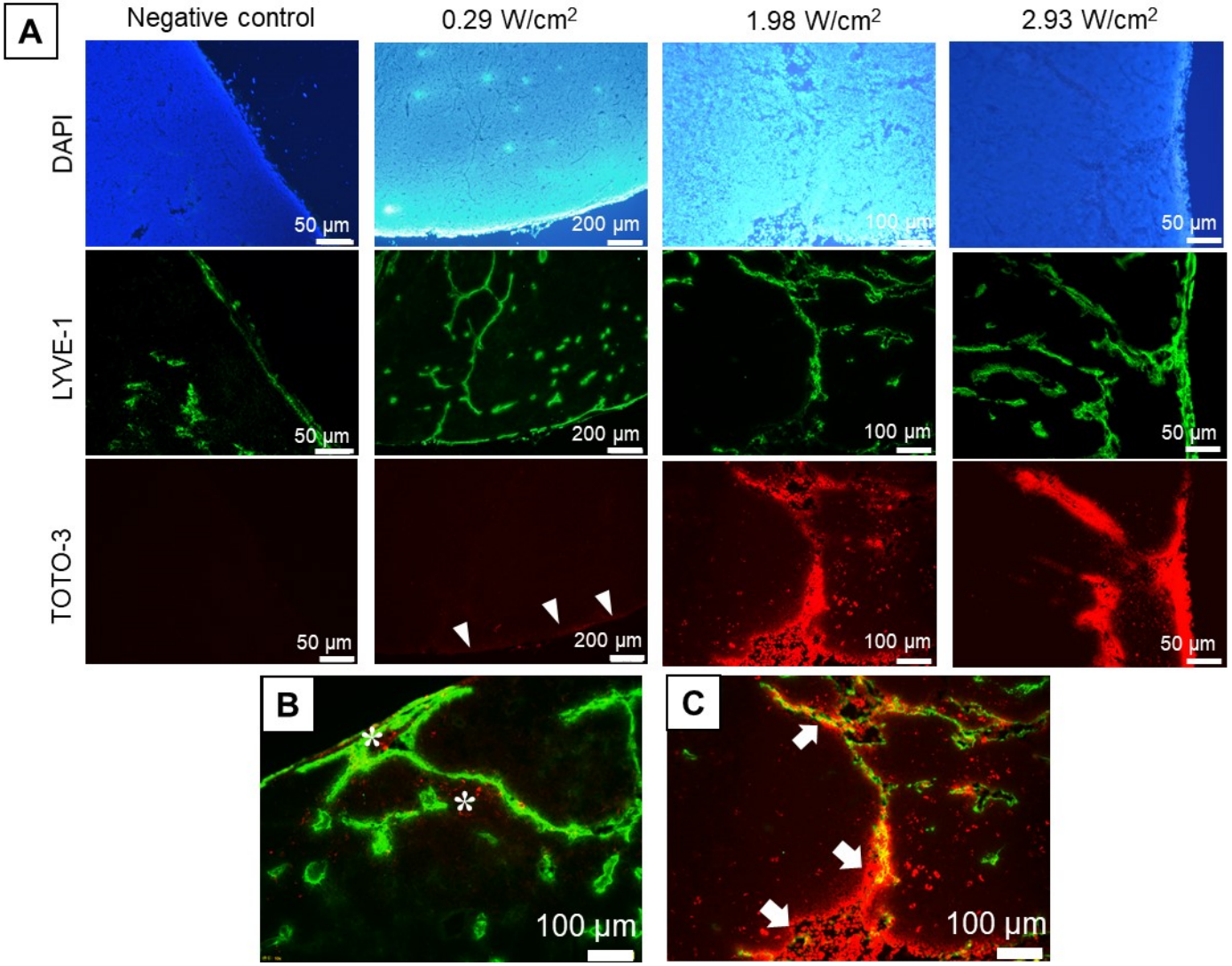
A
Negative control
0.29 W/cm2
1.98 W/cm2
2.93 W/cm2
DAPI
LYVE-1
TOTO-3
50 μm
200 μm
100 μm
B
C
100 μm

1

Figure 3

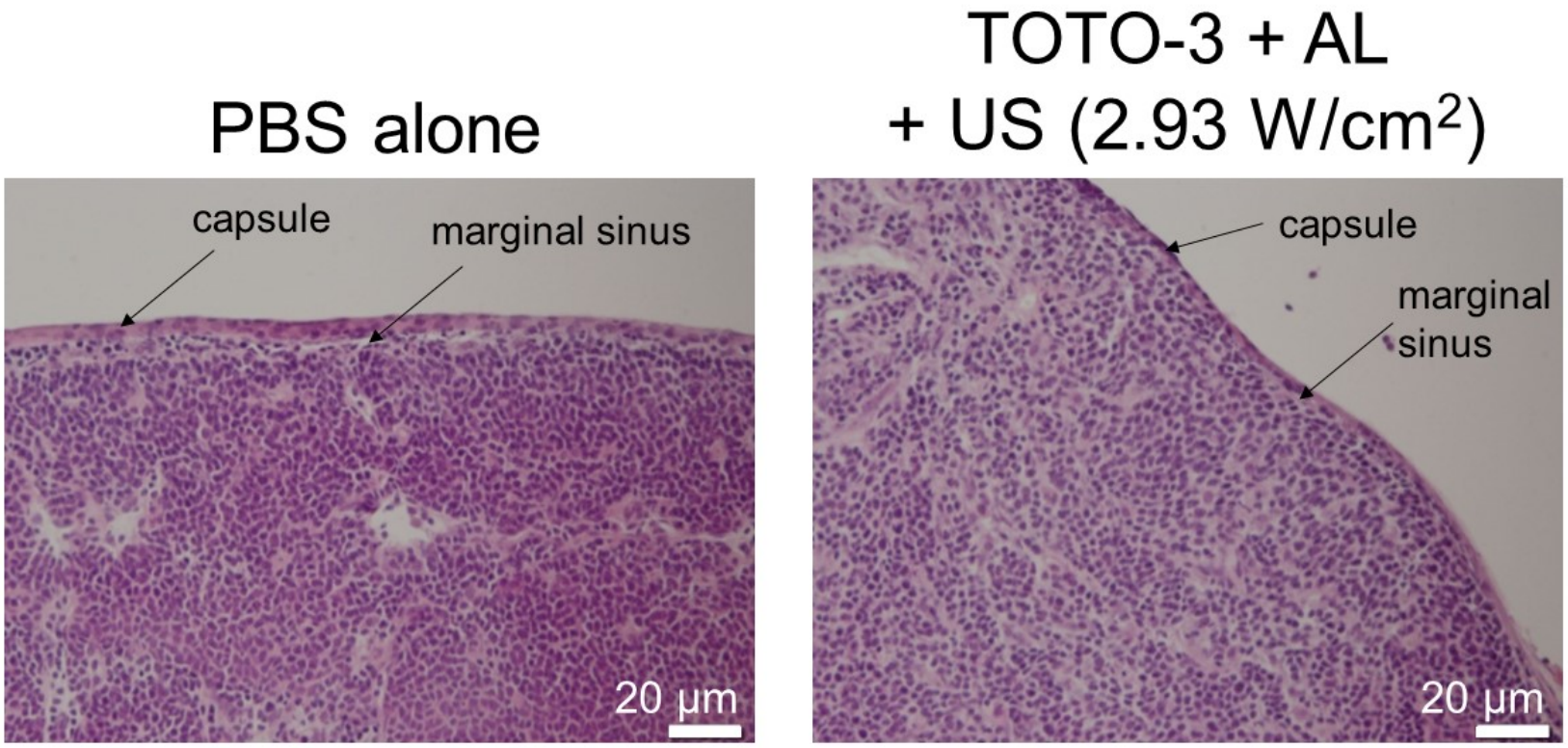
PBS alone
capsule
marginal sinus
20 μm
TOTO-3 + AL
+ US (2.93 W/cm2)
capsule
marginal
sinus
20 μm

Figure 4

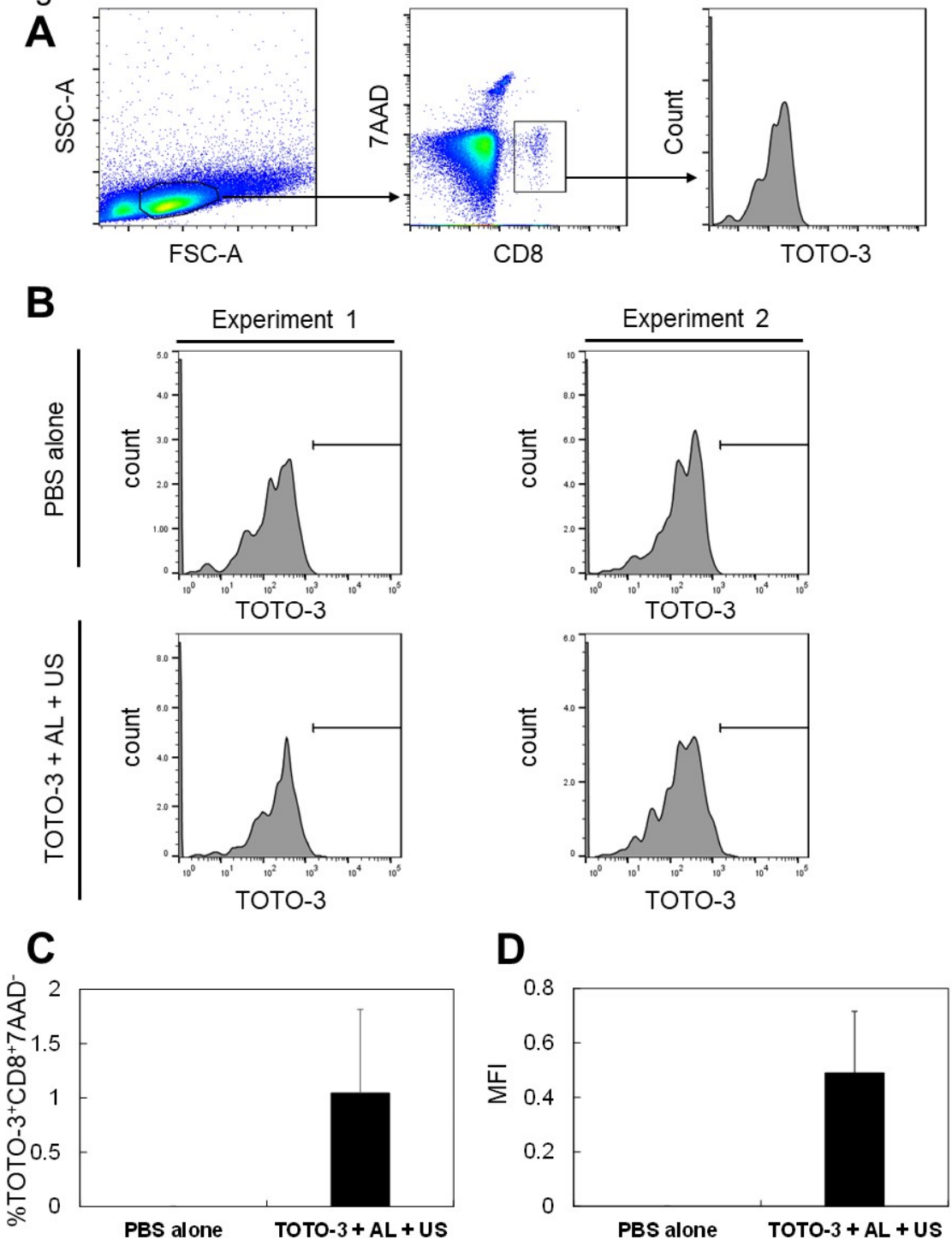
A
SSC-A
FSC-A
7AAD
CD8
Count
TOTO-3
B
Experiment 1
Experiment 2
PBS alone
TOTO-3 + AL + US
count
TOTO-3
C
%TOTO-3+CD8+7AAD-
PBS alone
TOTO-3 + AL + US
D
MFI
PBS alone
TOTO-3 + AL + US

Biochemical and Biophysical Research Communications

Declaration of competing interests

☒ The authors declare that they have no known competing financial interests or personal relationships that could have appeared to influence the work reported in this paper.

☐ The authors declare the following financial interests/personal relationships which may be considered as potential competing interests:

Please note that all *Biochemical and Biophysical Research Communications* authors are required to report the following potential conflicts of interest with each submission. If applicable to your manuscript, please provide the necessary declaration in the box above.

(1) All third-party financial support for the work in the submitted manuscript.
(2) All financial relationships with any entities that could be viewed as relevant to the general area of the submitted manuscript.
(3) All sources of revenue with relevance to the submitted work who made payments to you, or to your institution on your behalf, in the 36 months prior to submission.
(4) Any other interactions with the sponsor of outside of the submitted work should also be reported. (5) Any relevant patents or copyrights (planned, pending, or issued).
(6) Any other relationships or affiliations that may be perceived by readers to have influenced, or give the appearance of potentially influencing, what you wrote in the submitted work. As a general guideline, it is usually better to disclose a relationship than not.

Highlights

- We report a new method of foreign molecule delivery into mouse lymphocytes *in vivo*
- The method used lymphatic administration and sonoporation with acoustic liposomes
- TOTO-3 fluorophores (molecular weight: 1,355) were delivered into lymphocytes
- 1.93 W/cm^2 of 970-kHz ultrasound produced extravasation with minimal tissue damage
- This technique is a prospective novel approach for immunotherapy